PHYSICAL REVIEW D **95,** 015028 (2017)

Fundamental composite electroweak dynamics: Status at the LHC

Alexandre Arbey[*]
Centre de Recherche Astrophysique de Lyon, CNRS, UMR 5574, Saint-Genis-Laval Cedex F-69561, France

Giacomo Cacciapaglia,[†] Haiying Cai,[‡] Aldo Deandrea,[§] and Solène Le Corre[‖]
Univ. Lyon, Université Claude Bernard Lyon 1, CNRS/IN2P3, UMR5822 IPNL, F-69622 Villeurbanne, France

Francesco Sannino[¶]
CP^3-Origins and DIAS, University of Southern Denmark, Campusvej 55, DK-5230 Odense, Denmark
(Received 16 July 2016; published 30 January 2017)

Using the recent joint results from the ATLAS and CMS collaborations on the Higgs boson, we determine the current status of composite electroweak dynamics models based on the expected scalar sector. Our analysis can be used as a minimal template for a wider class of models between the two limiting cases of composite Goldstone Higgs and Technicolor-like ones. This is possible due to the existence of a unified description, both at the effective and fundamental Lagrangian levels, of models of composite Higgs dynamics where the Higgs boson itself can emerge, depending on the way the electroweak symmetry is embedded, either as a pseudo-Goldstone boson or as a massive excitation of the condensate. In our template, a mass term for the fermions in the fundamental theory acts as a stabilizer of the Higgs potential, without the need for partners of the top quark. We constrain the available parameter space at the effective Lagrangian level. We show that a wide class of models of fundamental composite electroweak dynamics are still compatible with the present constraints. The results are relevant for the ongoing and future searches at the Large Hadron Collider.

DOI: 10.1103/PhysRevD.95.015028

I. INTRODUCTION

The discovery of the Higgs boson is a landmark that establishes on a firmer experimental ground the standard model (SM) of particle physics. More excitingly, however, this discovery constitutes an invaluable source of information to help unveiling a more fundamental theory of particle interactions. The SM, in fact, suffers from a number of theoretical and phenomenological shortcomings such as the absence of a mechanism stabilizing the electroweak scale against quantum corrections and of a dark matter candidate. For these reasons the SM can be seen as an effective description in search of a more fundamental one.

Despite the fact that a fully satisfactory underlying theory has yet to be found, it is however possible to use the new experimental information on the Higgs sector to constrain extensions of the SM, which render this sector at least more fundamental. We shall focus on the possibility that the Higgs sector of the SM is composed of a new fundamental strongly coupled dynamics. The Higgs particle could then naturally emerge in two ways: mostly as a pseudo-Nambu Goldstone boson (pNGB) [1,2]; or mostly as the first composite scalar fluctuation of the new fundamental fermion condensate of technicolor (TC) inspired theories. In general, it will be a linear combination of both states.

Although within an effective Lagrangian description these different realizations seem superficially different, in fact, at a more fundamental level one can show that any underlying four-dimensional composite pNGB nature of the Higgs is always accompanied by the TC limit. We should stress here that we will use the word technicolor to indicate any theory where the Higgs arises as a massive bound state of the dynamics, not associated with a spontaneously broken symmetry, without restriction to QCD-like underlying dynamics. These two deceivingly different phenomenological realizations of the Higgs (pNGB and TC) are, de facto, unified at the fundamental level [3]. They differ only in the final dynamical alignment of the electroweak symmetry and its embedding in the larger global symmetry of the fundamental theory. The converse is not true, i.e. one can have fundamental theories breaking the electroweak (EW) symmetry dynamically without admitting a pNGB Higgs limit.

The time-honored example of fundamental descriptions of composite Higgs theories is technicolor [4,5] where a scaled-up QCD dynamics was employed. The original Weinberg and Susskind TC models, unfortunately, suffer of a number of serious phenomenological shortcomings

[*]alexandre.arbey@ens-lyon.fr
[†]g.cacciapaglia@ipnl.in2p3.fr
[‡]hcai@ipnl.in2p3.fr
[§]deandrea@ipnl.in2p3.fr
[‖]s.le-corre@ipnl.in2p3.fr
[¶]sannino@cp3-origins.net

and are, therefore, not phenomenologically viable. Among these issues there is the fact that the lightest massive composite scalar of the theory, the $\sigma(600)$, when scaled up to the electroweak scale has a mass of around 1.5 TeV that can hardly be reconciled with experiments [6]. Constraints on TC models coming from the flavor sector must be taken *cum grano salis* because they assume knowledge of extra, yet unspecified, sectors needed to endow the SM fermions with mass. The interplay of these sectors with the one responsible for breaking the electroweak symmetry typically modifies the constraints [7–10]. The issue of flavor has also been analyzed in the context of extra dimensional setups (see for instance [11,12]), which however cannot be considered on the same footing as fundamental theories [13]. Recently, analyses using crossing symmetry in conformal field theories have added extra constraints for the scalar operator with the lowest dimension [14,15] hinting that the scenario with bilinear 4-fermion interactions may be unlikely. However, the constraints may not be necessarily applicable to the operator relevant for flavor [16]. For an analysis concerning this issue see [17] and references therein. In the following we shall not consider the problem of flavor as it would require us to go beyond the effective description used in this paper and is anyway an open problem in particle physics.

Technicolor shortcomings are not generalizable to other fundamental models of composite dynamics [6]. There is, in fact, a vast number of possible underlying theories at our disposal [18–24] that can be used to break the electroweak symmetry dynamically. For these theories the phenomenological constraints of Weinberg and Susskind TC models do not automatically apply, the reason being that the resulting composite dynamics can be very different from QCD. In particular modern models of fundamental dynamical electroweak symmetry breaking are based on the use of both different gauge groups and different underlying fermionic matter representations, as summarized in [6]. It is therefore important to test these new fundamental theories against data, especially because these models have the ambition to use a more fundamental nature of the Higgs boson and its sector. Similarly the composite Higgs of pNGB nature, if realized in nature beyond an effective description, should also be related to an underlying composite dynamics [25].

Following the results of [3] we wish to determine the experimental status, via an effective Lagrangian approach, of the scalar sector of theories unifying the composite pNGB and Techni-Higgs at a more fundamental level. The physical 125 GeV Higgs boson is therefore identified with the lightest state of the theory which is generically a mixture of a composite pNGB and the Techni-Higgs state. The construction of the effective Lagrangian will be strongly based on the existence of an underlying theory, in terms of the allowed symmetries and expected properties of the bound states. This approach complements the modern take on composite Higgs models, which was originally inspired from models in warped extra dimensions [26]. For a review of the vast literature on minimal, and nonminimal, models, we refer the readers to the Refs. [27–29].

Although we are not using QCD as a template for our model building, it is a fact that it contains in its spectrum a plethora of composite states, i.e. pNGBs, massive (pseudo)scalar resonances, axial and vector states, baryons (composite fermions) as well as higher spin states. Even if the composite dynamics is not QCD-like, a *smoking gun* evidence that new fundamental composite dynamics drives electroweak symmetry breaking would be the discovery of new composite states.

Typically the phenomenology of nonperturbative extensions of the SM is limited to the bottom-up approach that lacks, however, of specific predictions, for example for the actual spectrum of particles to be discovered, relevant to guide experimental searches. One would, in fact, like to have realistic expectations on when new states will be discovered at colliders. In Refs. [30,31] a minimal realization in terms of an underlying gauge theory was provided consisting in a new underlying fundamental composite dynamics (FCD), i.e. $\mathrm{SU}(2)_{\mathrm{FCD}}$ gauge theory with two Dirac fundamental fermions transforming according to the defining representation of the gauge group. The symmetry breaking pattern $\mathrm{SU}(4)/\mathrm{Sp}(4)$ thus emerges as the minimal scenario, while less minimal cases typically contain additional light pNGB scalars. Our analysis will make use of the parametrization discussed in [3], and of the recent LHC results, to establish the status of this class of theories. We will focus on the scalar sector, which is expected to encompass the lightest states within the reach of the LHC. In particular we discuss the fine tuning issue in the alignment and Higgs mass, and we address the impact on the parameter space from the 125 GeV Higgs coupling measurements. At the same time, we revisit the bounds from the electroweak precision tests (EWPTs) by including the effect of a Techni-Higgs, thus allowing to study both the pNGB and the technicolor limits in a unified way. Finally we discuss the direct LHC constraints on the singlet pNGB and on the heavier Higgs, present in the spectrum.

The nonperturbative chiral dynamics of this theory is also being studied via first principle lattice simulations with noteworthy results. We know now, for example, that the pattern of chiral symmetry breaking that we shall be using below, i.e. SU(4) to Sp(4), occurs dynamically [32–34]. Even though this result was not unexpected, we consider a confirmation by first principle calculation as being an essential validation for the theory, before it can be confidently used for phenomenological applications. Recently the spectrum of the lightest spin-one states appeared in [33–35]. The lattice results on the spin-1 spectrum are very important for the phenomenology of this class of models, as it points to very heavy spin-1 states (especially in the pNGB Higgs limit), and thus motivates us to focus on the perspectives to discover the lighter scalar sector of the

theory. Equally important lattice results for the spectrum of minimal fundamental models of dynamical electroweak symmetry breaking that do not admit a composite pNGB Higgs limit are being produced with fermions in the adjoint representation [6]. Direct experimental searches for these models have recently appeared in [36].

The paper is structured as follows: in Sec. II we recap the main features of the model. The bounds from electroweak precision measurements and the Higgs couplings are presented in Sec. III, while in Sec. IV we show the experimental bounds on the heavier Higgs. Finally, in Sec. V we discuss the prospects to observe the lightest new particle, the singlet η, at the LHC and at a Linear Collider, before concluding in Sec. VI.

II. THE MODEL

In this paper we focus on a unified and minimal description of composite pNGB Higgs and TC models stemming from the simplest realization in terms of an underlying fundamental dynamics. Here, by simplest, we mean that it is based on the smallest asymptotically free gauge group with the smallest number of fermions needed for model building. The model, first presented in [30,31], relies on a gauge $\mathrm{SU}(2)_{\mathrm{FCD}}$ strongly coupled group with just two Dirac fermions transforming according to the fundamental representation of the underlying gauge group.[1] Since the representation is pseudoreal, the new fermions can be described as 4 Weyl fermions Q^i, so that the global symmetry of the fermionic sector is SU(4). The additional classical U(1) global symmetry is anomalous at the quantum level.[2] Because SU(2) can be viewed as the first of the symplectic groups [20] the phenomenological analysis, and model building can be generalised to $\mathrm{Sp}(2N)_{\mathrm{FCD}}$ [39].

The underlying Lagrangian is

$$\mathcal{L} = -\frac{1}{4} F^a_{\mu\nu} F^{a\mu\nu} + \bar{Q}_j (i\sigma^\mu D_\mu) Q_j - M_Q^{ij} Q_i Q_j + \mathrm{H.c.} \quad (1)$$

with $F^a_{\mu\nu}$ the field strength of the FCD group, and M_Q is a general mass matrix. First principle numerical simulations [32–34] have demonstrated that the $\mathrm{SU}(2)_{\mathrm{FCD}}$ model does lead to a fermion condensate in the chiral limit breaking the global symmetry $\mathrm{SU}(4) \to \mathrm{Sp}(4)$. The group-theoretical properties of the condensate are

$$\langle Q^i Q^j \rangle = \mathbf{6}_{\mathrm{SU}(4)} \to \mathbf{5}_{\mathrm{Sp}(4)} \oplus \mathbf{1}_{\mathrm{Sp}(4)}, \quad (2)$$

transforming as a 2-index antisymmetric representation of SU(4). The coset space $\mathrm{SU}(4)/\mathrm{Sp}(4)$ is parametrized by 5 Goldstone bosons, transforming as a $\mathbf{5}$ of Sp(4) [40,41].

[1]This model was first proposed as a UV completion of little Higgs models in [37].

[2]The physical consequences are interlaced with the possible addition of the topological gauge-term [38].

We need now to specify the embedding of the electroweak symmetry in the model: the simplest choice is to assign the first two Q^i to a doublet of $\mathrm{SU}(2)_L$, and the second two to a doublet of $\mathrm{SU}(2)_R$ (the diagonal generator of $\mathrm{SU}(2)_R$ being the generator of hypercharge). In this way, all gauge anomalies vanish, and we can keep track explicitly of the custodial symmetry built in the model. Another point is that with this embedding, we can choose an alignment of the condensate in SU(4) that does not break the EW symmetry: this direction is in fact determined by the mass matrix M_Q. The most general gauge-invariant mass term can be written as:

$$M_Q = \begin{pmatrix} \mu_L i\sigma_2 & 0 \\ 0 & \mu_R i\sigma_2 \end{pmatrix}, \quad (3)$$

where σ_2 is the second Pauli matrix, and the phases of the techniquarks can be used to make the two parameters $\mu_{L/R}$ real. This mass term explicitly breaks SU(4) to Sp(4) in the case where $|\mu_L| = |\mu_R|$. In the following, we will choose $\mu_R = -\mu_L$ in order to use the same alignment of the vacuum as in [3], however the sign choice is arbitrary and irrelevant as it can always be reversed by a change in the phase of the constituent quarks. All the physical results, therefore, are independent on the phases appearing in the mass matrix and in the condensate, provided we do not include the topological term [38]. The EW preserving vacuum, aligned with the mass matrix, is therefore

$$\Sigma_B = \begin{pmatrix} i\sigma_2 & 0 \\ 0 & -i\sigma_2 \end{pmatrix}. \quad (4)$$

A list of the 10 unbroken generators S^i and of the 5 broken ones X^j can be found in Ref. [3]. In this basis, the $\mathrm{SU}(2)_L$ generators are $S^{1,2,3}$, while the $\mathrm{SU}(2)_R$ ones are $S^{4,5,6}$. The alignment of the condensate can be changed by applying a SU(4) transformation generated by the 5 broken generators: as $X^{1,2,3,4}$ form a SU(2) doublet, one can use gauge transformations to align the vacuum along the Higgs direction (X^4 in our notation) without loss of generality. On the other hand, X^5 corresponds to a singlet of the gauged subgroup of SU(4), therefore a rotation along this direction will not change the physics of the model. Furthermore, it can be shown that a transformation $e^{i\theta' X^5}$ will generate a relative phase between the mass terms μ_L and μ_R of the two techniquark doublets: as already explained, this phase is irrelevant and can always be removed by a phase redefinition of the quarks. In other words, our choice to have real masses already fixed $\theta' = 0$. Introducing θ' in the vacuum alignment will therefore not add any new physical effects in the theory. The most general vacuum, therefore, can be written as:

$$\Sigma_0 = e^{i\gamma} e^{i\theta X^4} \cdot \Sigma_B = e^{i\gamma} \begin{pmatrix} \cos\theta i\sigma_2 & \sin\theta \mathbb{1}_{2\times 2} \\ -\sin\theta \mathbb{1}_{2\times 2} & -\cos\theta i\sigma_2 \end{pmatrix}. \quad (5)$$

The phase γ is generated by the anomalous U(1) symmetry, and it may therefore carry physical effects: in fact, it will generate CP violation in the chiral Lagrangian via the Pfaffian of the pion matrix [31]. In the following, for simplicity, we will limit ourselves to a CP-invariant model, thus setting $\gamma = 0$. The only free parameter θ aligns the condensate to a direction that does break the EW symmetry, and its value will be determined once quantum corrections are added.

Based on the above symmetry considerations, one can describe the physics of the 5 Goldstone bosons via the CCWZ formalism [42]: here we will use a linearly transforming matrix defined as

$$\Sigma = e^{i\sum_{j=1}^{5} Y^j \chi_j / f} \cdot \Sigma_0, \quad (6)$$

where χ_j are the pNGB fields, and $Y^j = e^{i\theta/2X^4} \cdot X^j \cdot e^{-i\theta/2X^4}$ are the broken generators in the Σ_0 vacuum. For our purposes, this formalism is completely equivalent to the one based on 1-forms. The chiral Lagrangian for this model has been studied in previous works [30,40,41,43,44], while the addition of the σ has been studied in [43] via the linear sigma-model (including vector and axial states) and in [3] for the nonlinear case reported here:

$$\begin{aligned} \mathcal{L}_{\mathrm{CCWZ}} = {} & \kappa_G(\sigma) f^2 \mathrm{Tr}[(D_\mu \Sigma)^\dagger D^\mu \Sigma] \\ & + \frac{1}{2}\partial_\mu\sigma\partial^\mu\sigma - \frac{1}{2}M^2\kappa_M(\sigma)\sigma^2 \\ & + f(\kappa_t(\sigma) y_u'^{ij} (Q_{L,i} u^c_{R,j})^\dagger_\alpha + \kappa_b(\sigma) y_d'^{ij} (Q_{L,i} d^c_{R,j})_\alpha \\ & + \kappa_l(\sigma) y_l'^{ij} (L_i l^c_j)^\dagger_\alpha) \mathrm{Tr}[P^\alpha \Sigma] + \mathrm{H.c.} \end{aligned} \quad (7)$$

where D_μ contains the EW gauge bosons, and we added the couplings of the Sp(4) singlet σ. The matrices P^α are spurions that project the pion matrix on its components transforming as a doublet of $\mathrm{SU}(2)_L$. As we shall see later, the σ can also play the role of the Higgs boson, even though naively its mass is expected to be large. The second line contains effective couplings of the condensate to the SM fermions. Such terms are necessary in order to give mass to the fermions in a similar way as Yukawa couplings do in the SM. A possible origin of such terms can be traced back to four-Fermi interactions in the form (for the up-sector):

$$\mathcal{L}_{\mathrm{EFCD}} = -\frac{y_u^{ij}}{\Lambda_u^2} (QQ)^\alpha (Q_{L,i} u^c_{R,j})^\dagger_\alpha + \mathrm{H.c.} \quad (8)$$

As all the Yukawa terms have the same 4-Fermi origin, one may expect $\kappa_t = \kappa_b = \kappa_l$. This operator emerges naturally in the chiral purely fermionic extended FCD theory of [45] or via integrating techniscalars in the extended FCD of [46] when taking their heavy limit.

A detailed analysis of this Lagrangian can be found in [3]: here we will limit ourselves to listing the main results relevant for the phenomenology of the scalar sector. First, the alignment of the vacuum generates masses for both the W and Z, as well as fermions:

$$\begin{aligned} m_W^2 &= 2g^2 f^2 \sin^2\theta = \frac{g^2 v^2}{4}, \qquad m_Z^2 = \frac{m_W^2}{\cos^2\theta_W}, \\ m_f &= y'_f f \sin\theta = \frac{y'_f v}{2\sqrt{2}}, \end{aligned} \quad (9)$$

where $v = 2\sqrt{2} f \sin\theta$, and the relation between the Z and W masses is guaranteed by the custodial symmetry. Additional small corrections arise from the singlet field σ acquiring a vacuum expectation value, however such corrections will be neglected in the following. Equation (7) also determines the couplings of the scalars, both pNGBs and σ, to the gauge bosons and SM fermions. First it should be said that the first 3 pions are exact Goldstone bosons and are eaten by the massive W and Z (for $\theta \neq 0$), so they can be removed in the Unitary gauge. About the remaining two pions, they are both pNGBs and, while one of them behaves like a Higgs boson in the sense that it couples linearly to the massive states, the other is a singlet and only couples quadratically. We can therefore rename the two as h and η:

$$\Sigma = e^{iY^4 h/f + iY^5 \eta/f} \cdot \Sigma_0. \quad (10)$$

Expanding Eq. (7) in the unitary gauge, one obtains

$$\begin{aligned} g_{hWW} &= \sqrt{2} g^2 f \sin\theta\cos\theta = g^{\mathrm{SM}}_{hWW} \cos\theta, \\ g_{hf\bar{f}} &= \frac{y'_f}{\sqrt{2}} \cos\theta = g^{\mathrm{SM}}_{hf\bar{f}} \cos\theta, \end{aligned} \quad (11)$$

while the couplings to the Z are determined by custodial invariance. Similarly, expanding

$$\kappa(\sigma) = 1 + \frac{\kappa^{(1)}}{4\pi f}\sigma + \frac{1}{2}\frac{\kappa^{(2)}}{(4\pi f)^2}\sigma^2 + \ldots \quad (12)$$

one finds the couplings of σ:

$$\begin{aligned} g_{\sigma WW} &= \frac{\kappa_G^{(1)}}{4\pi f} m_W^2 = g^{\mathrm{SM}}_{hWW} \tilde{\kappa}_G \sin\theta, \\ g_{\sigma f\bar{f}} &= \frac{\kappa_f^{(1)}}{4\pi f} m_f = g^{\mathrm{SM}}_{hf\bar{f}} \tilde{\kappa}_f \sin\theta, \end{aligned} \quad (13)$$

where we have defined

$$\tilde{\kappa}_G = \frac{\kappa_G^{(1)}}{2\sqrt{2}\pi}, \qquad \tilde{\kappa}_f = \frac{\kappa_f^{(1)}}{\sqrt{2}\pi},$$
$$\tilde{\kappa}_G^{(2)} = \frac{\kappa_G^{(2)}}{4\pi^2}, \qquad \tilde{\kappa}_f^{(2)} = \frac{\kappa_f^{(2)}}{2\pi^2}, \tag{14}$$

for later convenience. A summary of the couplings of the 3 scalars to the SM states normalized to the SM values can be found in Table I. It is also useful to complete the list with the couplings of two scalars to the fermions, which are absent in the SM but may be relevant for the pair production of the scalars at the LHC:

$$g_{hhf\bar{f}} = -\frac{m_f}{v^2}\sin^2\theta, \tag{15}$$

$$g_{\sigma\sigma f\bar{f}} = \frac{\kappa_f^{(2)}}{(4\pi f)^2} m_f = \tilde{\kappa}_f^{(2)} \frac{m_f}{v^2}\sin^2\theta, \tag{16}$$

$$g_{h\sigma f\bar{f}} = \frac{\kappa_t^{(1)}}{4\pi f}\frac{m_f}{v}\cos\theta = \tilde{\kappa}_f \frac{m_f}{v^2}\sin\theta\cos\theta, \tag{17}$$

$$g_{\eta^2 f\bar{f}} = -\frac{m_f}{v^2}\sin^2\theta. \tag{18}$$

The importance of such couplings for the Higgs pair production has been stressed in Ref. [47].

A. The Higgs spectrum and fine-tuning

The masses of the pNGBs are generated by operators that break explicitly the global symmetry both at tree and loop levels.

$$V_{\text{scalars}} = \kappa_G(\sigma)V_{\text{gauge}} + \kappa_t^2(\sigma)V_{\text{top}} + \kappa_m(\sigma)V_m. \tag{19}$$

The first two terms are generated by loops of the EW gauge bosons and the top, while the third comes from the mass term of the techniquarks, which explicitly breaks $\mathrm{SU}(4) \to \mathrm{Sp}(4)$. Here we will summarize the main results. To further simply the analysis we neglect the gauge boson contribution. This is justified by the fact that it is smaller than the top one. Also, we omit the contribution of σ to identify the symmetry breaking alignment with respect to the electroweak symmetry.

TABLE I. Coupling of one and two scalars to gauge bosons and fermions normalized to the SM value. The bilinear couplings to fermions are not reported here as they are absent in the SM.

	WW, ZZ	$f\bar{f}$
h	$\cos\theta$	$\cos\theta$
σ	$\tilde{\kappa}_G \sin\theta$	$\tilde{\kappa}_f \sin\theta$
η	…	…
hh	$\cos 2\theta$	
σh	$\tilde{\kappa}_G \sin 2\theta$	
$\sigma\sigma$	$\tilde{\kappa}_G^{(2)} \sin^2\theta$	
$\eta\eta$	- $\sin\theta^2$	

First, we can compute the potential for θ:

$$V(\theta) = y_t'^2 C_t \cos^2\theta - 4C_m \cos\theta + \text{constant} \tag{20}$$

where $C_{t,m}$ are order 1 coefficients determined by the dynamics (C_t is expected to be positive to match the sign of a fermion loop). The minimum of the potential is thus given by

$$\cos\theta_{\min} = \frac{2C_m}{y_t'^2 C_t}, \quad \text{for } y_t'^2 C_t > 2|C_m|. \tag{21}$$

Note that a small θ can only be achieved for $2C_m \to y_t'^2 C_t$: in order to reach the pNGB Higgs limit, one needs therefore to fine-tune two contributions in the potential which are of very different origins. This is the only severe fine-tuning required in the model, if a small θ needs to be achieved.[3] Note also that in the limit of a small mass for the technifermions, $C_m \ll C_t$, the vacuum moves towards the TC limit $\theta = \pi/2$. It is also noteworthy that here we use an explicit mass term for the techniquarks to stabilize the potential, while in other models of composite (pNGB) Higgs in the market the stabilization is due to quartic terms. Naively, quartic contributions from top loops are subleading corrections, however large contributions may arise due to the presence of light fermionic resonances who mix to the top as in models with top partial compositeness [49].

This potential also determines the masses of the pNGBs:

$$m_{\chi_{1,2,3}}^2 = \frac{f^2}{4}(2C_m - y_t'^2 C_t\cos\theta)\cos\theta = 0,$$
$$m_h^2 = \frac{f^2}{4}(2C_m\cos\theta - y_t'^2 C_t\cos(2\theta)) = \frac{y_t'^2 C_t f^2}{4}\sin^2\theta,$$
$$m_\eta^2 = \frac{f^2}{4}(2C_m\cos\theta + y_t'^2 C_t\sin^2\theta) = \frac{y_t'^2 C_t f^2}{4}, \tag{22}$$

where we have used the minimum condition to remove the dependence on C_m. We notice here that, as expected, the new fundamental elementary fermion mass term gives the same mass (of order f) to all pions. On the other hand, the top loop gives a mass of order f to the pNGB Higgs, and a mass of order $f\sin\theta$ to the EW singlet. This can be easily understood: the top couples via 4-fermi interactions to the techniquarks doublet that transforms as a doublet of SU(2), thus the top loop will generate the usual divergent

[3] A very different case is the realization where a pNGB Higgs is elementary [48]. The pNGB Higgs is not fine-tuned in terms of the parameter θ (even if the hierarchy problem persists), as the corrections to the potential, once the quadratic divergences are subtracted, are in the fourth power of the couplings (corresponding to logarithmic corrections to the quartic coupling).

contribution to its mass that, following naive dimensional analysis, can be approximated as

$$\Delta m_h^2(\text{top}) = C\frac{y_t'^2}{16\pi^2}\Lambda^2 = C y_t'^2 f^2. \tag{23}$$

This large contribution, however, is canceled by the contribution of the explicit mass at the minimum, so that the final value of the pNGB Higgs mass is

$$m_h^2 = \frac{y_t'^2 C_t f^2}{4}\sin^2\theta = m_\eta^2 \sin^2\theta = \frac{C_t m_{\text{top}}^2}{4}. \tag{24}$$

Note that it would be enough to have $C_t \sim 2$ to generate the correct value for the Higgs mass. The value of C_t is not a free parameter, but it can be determined by the dynamics. At present, no calculation of such coefficients is available. Nevertheless, no additional fine-tuning is in principle necessary for the Higgs mass, once the fine-tuning in the alignment is paid off. The relation between the masses of h and η [31] also survives after the gauge corrections are included, however it can easily be spoiled by other corrections, like for instance the mixing between h and σ. Finally, the pions eaten by the W and Z are massless on the correct vacuum, as expected for exact Goldstone bosons. We should also stress that the relation between the Higgs and η mass are true in models where the stabilization of the potential is mainly due to the technifermion mass, while in cases with top partners it will depend on the details of the pre-Yukawa structures [41].

The parametric smallness of the pNGB Higgs mass can also be understood in terms of symmetries. The 3 Goldstone bosons eaten by W and Z are always massless, for any value of θ. Therefore, if we go continuously to the limit $\theta \to 0$, where the EW symmetry is restored, the mass of the pNGB Higgs must also vanish in order to reconstruct a complete massless SU(2) doublet. The same argument cannot be applied to η, which is a singlet unrelated to EW symmetry breaking.

In the natural presence of the singlet σ the spectrum is affected. In fact, σ mixes with h (but not with η), as they share the same quantum numbers. A detailed description of the mass matrix can be found in [3]. Here, we will keep the discussion general, so we will simply replace h and σ by the mass eigenstates $h_{1,2}$, where the lighter states h_1 is identified with the observed Higgs at $m_{h_1} = 125$ GeV:

$$\begin{pmatrix} h_1 \\ h_2 \end{pmatrix} = \begin{pmatrix} c_\alpha & s_\alpha \\ -s_\alpha & c_\alpha \end{pmatrix}\begin{pmatrix} h \\ \sigma \end{pmatrix}. \tag{25}$$

Both the mass m_{h_2} and the mixing angle α will be considered here as independent free parameters. It should only be reminded that $\alpha \to 0$ for $\theta \to 0$, as the EW symmetry is not broken in that limit, and also $\alpha \to \pi/2$ for $\theta \to \pi/2$ as a global U(1) subgroup will prevent mixing in the TC limit [30] (and we need to associate the observed Higgs with σ). The sign of α is not determined, however the analysis in [3] shows that the mass of the light state will generically receive a negative correction from the mixing, that is reduced with respect to the prediction in Eq. (23). We can therefore consider that

$$m_\eta \geq \frac{m_{h_1}}{\sin\theta}. \tag{26}$$

In the phenomenological results of Sec. V, we will assume the equality as a limiting scenario.

B. Trilinear scalar self-interactions

We present here the trilinear couplings among scalars, which are relevant for the pair production of the discovered Higgs[4]

$$g_{h^3} = \frac{3m_h^2}{v}\cos\theta, \tag{27}$$

$$g_{\sigma h^2} = -\frac{m_h^2}{v}\frac{1}{\sin\theta}(\tilde{\kappa}_m^{(1)}\cos^2\theta - 2\tilde{\kappa}_t\cos(2\theta)), \tag{28}$$

$$g_{\sigma^2 h} = \frac{m_h^2}{v}\frac{2\cos\theta}{\sin\theta}(\tilde{\kappa}_m^{(2)} - (\tilde{\kappa}_t^{(2)} + \tilde{\kappa}_t^2)), \tag{29}$$

and of η:

$$g_{h\eta^2} = \frac{m_h^2}{v}\cos\theta, \tag{30}$$

$$g_{\sigma\eta^2} = -\frac{m_h^2}{v}\frac{1}{\sin\theta}(\tilde{\kappa}_m^{(1)}\cos^2\theta + 2\tilde{\kappa}_t\sin^2\theta), \tag{31}$$

where we defined, for convenience,

$$\tilde{\kappa}_m^{(1)} = \frac{\kappa_m^{(1)}}{\sqrt{2}\pi}, \qquad \tilde{\kappa}_m^{(2)} = \frac{\kappa_m^{(2)}}{2\pi^2}, \tag{32}$$

and we are working in the nondiagonalized scalar basis.

It is interesting to notice that the couplings of σ diverge for small θ: this is a sign that they are proportional to the condensation scale f and thus increase for increasing condensation scale. The trilinear coupling of σ cannot be determined as it comes directly from the strong dynamics. It should therefore be considered as an additional free parameter, also proportional to the condensation scale f.

[4]The couplings are proportional to the pNGB mass m_h and not to the physical Higgs mass m_{h_1}. Thus these couplings should be compared to the SM value $g_{h^3}^{\text{SM}} = 3m_{h_1}^2/v$.

C. Flavor and lattice predictions

The construction of a realistic flavor sector has always been the main challenge in models of EW symmetry breaking via strong dynamics. In fact, while masses of gauge bosons can naturally arise via minimal gauging of the confining sector, the couplings to the SM fermions need to arise from effective couplings (like 4-fermion interactions) generated externally to the strong dynamics. The simplest mechanism is to imagine the presence of an extended gauge sector that generated 4-fermion interactions once the heavy gauge bosons are integrated out [50]. However, one would naively expect large flavor changing neutral currents (FCNCs) and difficulties in generating hierarchies in the Yukawa sector. One alternative is the possibility to generate only linear couplings in the so-called partial compositeness scenario [51]. The latter has been gaining popularity, as such mechanism can be easily implemented in extra dimensional models [11]. However, without specifying the origin of the flavor mixing, it is difficult to analyze the validity of the various proposals.

In this paper, we will not attempt to give a full solution to the flavor issue. The couplings to fermions we listed in the above formulas are rather generic and can be obtained independently on the specific origin of the effective Yukawa couplings. On the other hand, we should remark that, once a fundamental dynamical model is specified, the question of the origin of flavor interactions can be fully addressed. One possible way out to the old lore of the presence of FCNCs, is to assume that the masses of different fermion generations are induced at different scales. This scenario has been recently considered in an effective approach in Refs. [52–54]. It has also been shown that, in the minimal model under consideration based on a gauged $\mathrm{SU}(2)_{\mathrm{FCD}}$, the mass of the top alone can be generated by an extended gauge sector [45], thus providing a first bookkeeping example. In the case of partial compositeness, the solution of the flavor puzzle is strongly based on the assumption that the theory is conformal in the UV and that the hierarchies in the effective Yukawas are generated by large anomalous dimensions. In principle, scenarios of this kind can be obtained in a FCD approach [55–57], even though achieving fermionic bound states (top partners) with large anomalous dimensions is difficult [58]. However, very recently an alternative complete microscopic solution to the fermion mass generation in models of dynamical electroweak symmetry breaking has been put forward [46].[5] The novelty with respect to earlier approaches is in the introduction, along with the technifermions, of a minimal set of nonsupersymmetric techniscalars gauged under the underlying fundamental composite gauge group. The minimal set of scalars allows to introduce the correct SM flavor structure via renormalizable operators involving a SM fermion and a composite baryon made by a technifermion and a techniscalar, thus fully realizing the partial compositeness scenario microscopically. By construction, the scenario does not require large anomalous dimensions for the composite operators and lends an interesting flavor structure in which the underlying Yukawa structure emerges as a minimal *square root* of the SM Yukawa one. Furthermore one can argue that more involved approaches making use, for example, of only fundamental fermions because of the need for very large anomalous dimensions will resemble at some intermediate energy the construction in [46] albeit with the scalars seen as intermediate composite fields. The underlying model for the fermion sector used here naturally fits the construction of [46].

As already mentioned, here we will keep a pragmatic approach and therefore we will only rely on minimal couplings of the SM fermions to the strong dynamics: we believe that our results can therefore be easily applied to any specific mechanism generating the fermion masses.

Another remarkable feature of models based on a FCD is that they can be studied nonperturbatively on the lattice. Thanks to the vast progress in lattice technology, faster and more reliable calculations are now available compared to the early days of composite Higgs theories. In particular, the dynamics of the minimal model with $\mathrm{SU}(2)_{\mathrm{FCD}}$ and 2 Dirac fermions in the fundamental representation has been studied in detail [32–35]. The results clearly show that the spin-1 resonances are expected to be very heavy, with masses of the vector and axial states equal to

$$m_\rho = \frac{3.2 \pm 0.5}{\sin\theta}\ \mathrm{TeV}, \qquad m_a = \frac{3.6 \pm 0.9}{\sin\theta}\ \mathrm{TeV}. \tag{33}$$

In terms of the condensation scale $F_\pi = v/\sin\theta = 2\sqrt{2}f$, $m_\rho/F_\pi = 13.1 \pm 2.2$ and $m_a = 14.5 \pm 3.6$. Even though the phenomenology of such states is potentially very rich and interesting [59], the masses on the lattice show that they might be more relevant for a 100 TeV collider than for the LHC. Other physically relevant quantities that can be extracted form the lattice are related to the masses of the pNGBs (including the Higgs), i.e. the coefficients C_m and C_t that appear in the potential discussed in Sec. II A. Comparing the results at finite techniquark mass in [35] with the masses calculated above, we obtain[6]

[5]This is not an attempt to solve the naturalness problem, as fundamental scalars would also introduce a naturalness problem related to their mass, it is a framework where composite dynamics, albeit still of unnatural nature, is able to give masses to all the SM fermions via a partial composite scenario.

[6]Comparing the value of the pNGB mass at $\theta = 0$, $m_\pi^2 = C_m/16F_\pi^2$ with the lattice parametrization $m_\pi^2 = 2Bm_f$, we obtain $C_m = 32B/F_\pi m_f/F_\pi$, where $\omega_0^\chi B = 2.88 \pm 0.15 \pm 0.17$ and $\omega_0^\chi F_\pi = 0.078 \pm 0.004 \pm 0.012$ [35] (ω_0^χ is a normalization factor that drops out in physical quantities).

$$C_m = 1.2 \times 10^3 \frac{m_f}{F_\pi}. \tag{34}$$

As at the minimum of the potential one needs $C_m \sim 1$, the technifermion mass should have values $m_f \sim 10^{-3} F_\pi \sim$ GeV, which are consistently lower than the condensation scale. The coefficient C_t can be computed by evaluating on the lattice the correlator containing the insertion of a 4-fermion operator originating from a loop of tops. This simple calculation contrasts with the much more complex procedure that would be needed in theories with partial compositeness [60]. We would also like to mention that the mass of the techni-Higgs σ can also be computed, even though technically more difficult. Preliminary results point toward masses below the spin-1, but still very heavy. Noteworthy, lattice results in other models have shown that the σ can become lighter if the model contains heavy flavor that make the strong dynamics near conformal at higher energy scales [61], while other masses are much less affected.

D. Bounds from EWPTs

The precise determination of the oblique corrections is a delicate issue in composite extensions of the SM. A well-defined procedure must be employed that allows us to clearly disentangle the intrinsic contribution stemming from strong dynamics from the one coming from the genuine SM contribution. Once such a procedure is established, an estimate from the strongly coupled sector is needed. First principle lattice simulations are the primary method to determine this contribution. However, as a very rough estimate, one can use the one-loop contribution from the fundamental fermions with heavy constituent mass terms. In this case for one $\mathrm{SU}(2)_L$ doublet we have $\Delta S = 1/(6\pi)$. In the fundamental model under consideration, this translates into the following contribution

$$\Delta S_{\mathrm{UV}} = \frac{\sin^2\theta}{6\pi} \tag{35}$$

for each fundamental doublet.[7] The reason for the presence of the $\sin^2\theta$ term can be understood in terms of symmetries: in the radial composite Higgs limit $\theta \to \pi/2$, the fundamental fermions pick up a dynamical mass from the condensate which is aligned with the EW breaking direction, thus the calculation satisfies some of the assumptions in [64]; on the other hand, in the limit $\theta \to 0$, the EW symmetry is recovered and the S parameter must vanish. The power is understood in terms of masses: in fact, it is expected to be proportional to the square of the ratio of the dynamical mass aligned to the EW breaking direction, $\sim f \sin\theta$, and the total dynamical mass of the fermions, $\sim f$. This expectation is also confirmed by an operator analysis of this contribution, as shown in [31]. The strongly interacting contribution to the T parameter vanishes because the dynamics respects the $SU(2)_V$ custodial symmetry.

The underlying strong dynamics contribution must then be matched with the important one coming from the quantum corrections in the effective Lagrangian for the lightest states considered here. We will use a more naive way to estimate the total correction: we explicitly include the contribution of the loops of the lightest composite states,[8] i.e. the 125 GeV Higgs h_1, which contributes due to the modified couplings to gauge bosons, and the heavier "Higgs" h_2. Then, we will assume that the contribution of the heavier resonances can be approximated by the techni-quark loop in Eq. (35), as one would expect if the contribution were dominated by the lightest vector and axial resonances. The net effect can be estimated starting from the contribution of the Higgs loops and summarize the results in the following:

$$\begin{aligned}
\Delta S &= \frac{1}{6\pi}\left[(1-k_{h_1}^2)\ln\frac{\Lambda}{m_{h_1}} - k_{h_2}^2 \ln\frac{\Lambda}{m_{h_2}} + N_D \sin^2\theta\right], \\
\Delta T &= -\frac{3}{8\pi\cos^2\theta_W}\left[(1-k_{h_1}^2)\ln\frac{\Lambda}{m_{h_1}} - k_{h_2}^2 \ln\frac{\Lambda}{m_{h_2}}\right],
\end{aligned} \tag{36}$$

where

$$\begin{aligned}
k_{h_1} &= \cos(\theta-\alpha) + (\tilde{\kappa}_G - 1)\sin\theta\sin\alpha, \\
k_{h_2} &= \sin(\theta-\alpha) + (\tilde{\kappa}_G - 1)\sin\theta\cos\alpha,
\end{aligned} \tag{37}$$

and N_D is the number of technifermion doublets ($N_D = 2$ for $\mathrm{SU}(2)_{\mathrm{FCD}}$, and $2N$ for $\mathrm{Sp}(2N)_{\mathrm{FCD}}$). In this analysis we assumed the presence of physical cutoff Λ to be identified with the next massive state. The dependence on the cutoff emerges because the scalar loop contributions are divergent, as a sign of the effective nature of the Lagrangian. The divergence is corrected once the proper matching to the underlying UV dynamics is taken into account. In our phenomenological estimates, we will use

$$\Lambda = 4\pi f = \frac{\sqrt{2}\pi v}{\sin\theta}, \tag{38}$$

which is very close to the mass of the spin-1 resonances as shown by first-principle lattice simulations [32–34,65]. We also added to ΔS the naive strongly coupled contribution

[7] We note that this estimate is modified when the underlying dynamics is near conformal because of the violation of the second Weinberg's sum rule [62]. There is a limit, however, when this estimate turns into a precise result. This occurs close to the upper limit of the conformal window [63] provided the correct kinematical limits are chosen.

[8] The η does not contribute: in fact, its couplings can only generate corrections to the masses and, because of the custodial symmetry, such corrections do not enter the T parameter.

that should partially take into account the heavier states. This estimate is clearly naive but should capture at least the correct order of magnitude of the corrections. It should be stressed that a more appropriate calculation should be employed if one wanted to use lattice calculations of the contribution of the strong dynamics to S, where one finds also the discussion of the needed counterterms in the effective Lagrangian.

III. CONSTRAINTS FROM THE HIGGS COUPLING MEASUREMENTS AND EWPTS

The couplings of the Higgs boson have been measured by the LHC Collaborations ATLAS and CMS in a series of papers [66–71], which can be used to extract the constraints from the Higgs couplings. In the following we use the most recent combined results given by the two collaborations in a joint effort [72]. The results of the experimental analyses are provided as exclusion contours in terms of signal strengths, and treated in the way described in [73]. These experimental plots represent regions allowed at 68% confidence level (C.L.) by the analyses, in the plane of cross sections rescaling factors for the main Higgs decay channels $H \to \gamma\gamma$, WW^*, ZZ^*, $\bar{\tau}\tau$, $\bar{b}b$, under the assumption that W and Z-strahlung (VH) and vector boson fusion (VBF) modes are rescaled by the same factor, as well as the gluon fusion and $t\bar{t}H$. We fitted these lines as ellipses, therefore extrapolating the χ_i^2 for each channel as a paraboloid, i.e. approximating the likelihood functions with a Gaussian. The 2 dimensional likelihood for each channel, neglecting the $t\bar{t}H$ contribution, is given by:

$$\chi_i^2 = \begin{pmatrix} \mu^i_{ggH} - \hat{\mu}^i_{ggH} \\ \mu^i_{\mathrm{VBF/VH}} - \hat{\mu}^i_{\mathrm{VBF/VH}} \end{pmatrix}^T \cdot M_i^{-1} \cdot \begin{pmatrix} \mu^i_{ggH} - \hat{\mu}^i_{ggH} \\ \mu^i_{\mathrm{VBF/VH}} - \hat{\mu}^i_{\mathrm{VBF/VH}} \end{pmatrix}, \tag{39}$$

where $(\hat{\mu}^i_{ggH}, \hat{\mu}^i_{\mathrm{VBF/VH}})$ is the center of each ellipse and M_i is a symmetric matrix encoding information about its axes. In our model, we define the signal strengths to be:

$$\mu^i_{ggH} = \frac{\sigma_{ggH}(k_t^2, k_b^2)}{\sigma_{ggH,\mathrm{SM}}} \times \frac{k_i^2}{\sum_m k_m^2 \mathrm{Br}_m^{\mathrm{SM}}},$$
$$\mu^i_{\mathrm{VBF/VH}} = k_W^2 \times \frac{k_i^2}{\sum_m k_m^2 \mathrm{Br}_m^{\mathrm{SM}}}, \tag{40}$$

where those k_i^2s are rescaling factors for Higgs couplings with gauge bosons and fermions.

Through the χ^2 function we will determine the best fit point and we can then use the reconstructed quantity $\Delta\chi^2 = \chi^2 - \chi^2_{\mathrm{min}}$ to draw the exclusion limits. This method has been validated to reproduce the experimental results [74]. The bound from the EWPTs is taken from [75]: $S_{U=0} = 0.06 \pm 0.09$ and $T_{U=0} = 0.10 \pm 0.07$.

A. The composite pNGB Higgs limit

Here we assume σ to decouple and we identify the discovered Higgs with the pNGB h. This limit corresponds to the case $\alpha = 0$ and $\tilde{\kappa}_G = \tilde{\kappa}_t = 0$. In this limit both the Higgs couplings and EWPTs depend only on θ, thus allowing us to extract an upper bound on the value of this angle. The limits at 3σ are summarized in the following table:

	Higgs	$\mathrm{SU}(2)_{\mathrm{FCD}}$	$\mathrm{Sp}(4)_{\mathrm{FCD}}$	$\mathrm{Sp}(6)_{\mathrm{FCD}}$
$\theta <$	0.46	0.255	0.242	0.230

The numbers show that the bound from EWPTs (indicated by the symmetry group name) is much stronger than the bounds from the Higgs couplings (indicated as "Higgs"), and points to values $\sin\theta \lesssim 0.2$. This value is consistent with bounds obtained in other models of pNGB Higgs [76]. This result may seem trivial, however the methods employed to estimate the contribution of the strong dynamics are very different. While we use a simple technifermion loop, most results in the literature are based on the calculation of loops of spin-1 resonances [77,78] and often include the effects of loops of top partners [79]. From the values in the table, we also see that there is a mild dependence on the number of doublets in the dynamical model, thus signaling that the bound is dominated by the contribution of the Higgs boson.

In this analysis we ignored the presence of σ. However, one can imagine a situation where $\alpha \sim 0$ with a large value of $\tilde{\kappa}_G$. In this limit the mass eigenstate h_2 can therefore affect EWPTs. This situation can be achieved because the mixing between σ and h is mostly generated via the coupling of σ to the top and the mass term in the potential for the pNGBs, while the bounds are only sensitive to the coupling to gauge bosons. Even when the mixing vanishes the σ state still affects the EWPTs as shown in Fig. 1. Here we plot the upper bound on θ as a function of the mass of the heavier scalar mass for various values of $\tilde{\kappa}_G$. One can see that a nonzero value of the couplings can relax the bound if h_2 is light. Additional constraints arise form the measured couplings of the discovered Higgs and from direct searches on the heavier h_2 (the latter will be discussed in Sec. IV).

B. The technicolor limit

Another interesting limit occurs for $\theta = \pi/2$, i.e. the TC limit. In this case, the mixing vanishes and the Higgs is associated with σ, i.e. $\alpha = \pi/2$. The pNGB h decouples and, together with η, may play the role of dark matter [30], while the couplings of the 125 GeV Higgs depend on the details of the underlying dynamics and are associated to the $\tilde{\kappa}$ parameters. The correct value of the Higgs mass can be achieved via a cancellation between the dynamical mass, of the order of a TeV, and loop contributions from explicit breaking of the global

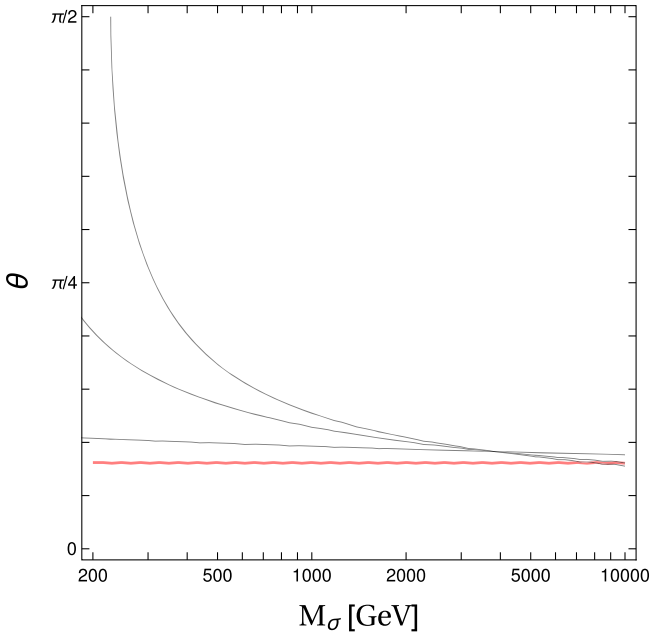

FIG. 1. Upper bound on θ as a function of the mass of σ. The red curve corresponds to the decoupling limit $\theta < 0.239$, while for the other lines correspond to $\tilde{\kappa}_G = 0.5$, 1 and 1.2, while we keep $\alpha = 0$ and $N_D = 2$.

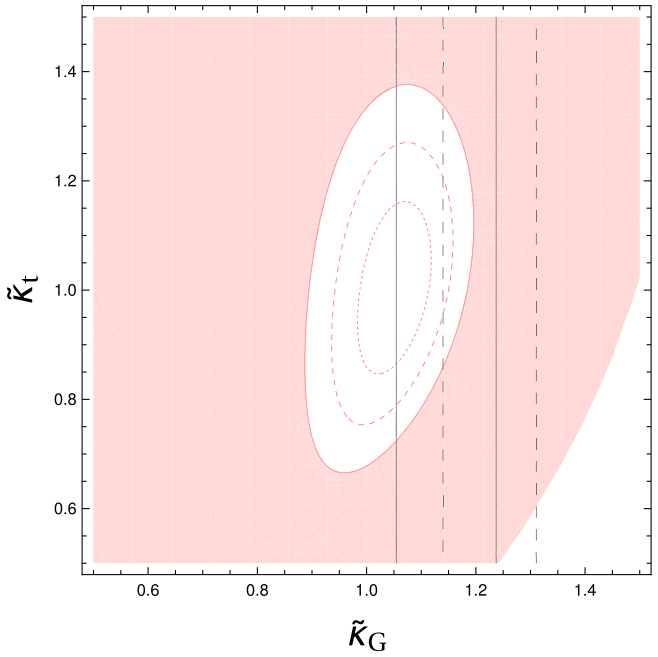

FIG. 2. Region allowed by the Higgs couplings in the TC limit $\theta = \alpha = \pi/2$, with 1, 2 and 3σ contours (combined CMS and ATLAS bounds). The regions within the vertical lines are allowed by EWPTs at 3σ for $\mathrm{SU}(2)_{\mathrm{FCD}}$ (solid) and $\mathrm{Sp}(4)_{\mathrm{FCD}}$ (dashed).

symmetry,[9] such as the top loops [10]. Assuming the mass gets the correct value, we can compute the bounds on the couplings of σ to gauge bosons $\tilde{\kappa}_G$ and fermions $\tilde{\kappa}_t$ (we are explicitly assuming that all fermions couple in the same way, i.e. $\tilde{\kappa}_t = \tilde{\kappa}_b = \tilde{\kappa}_l$). The results are shown in Fig. 2, where we plot 1, 2 and 3σ contours from the measured Higgs couplings. A fairly large region around the SM limit $\tilde{\kappa}_G = \tilde{\kappa}_t = 1$ is still open. In principle, there is no reason for these couplings to be close to the ones of the SM Higgs, however it is fascinating that this happens for the σ meson in QCD [82]. We also compare this allowed region with the bound from EWPTs, which is only dependent on $\tilde{\kappa}_G$. The vertical lines delimit the allowed region for two choices of N_D, corresponding to $\mathrm{SU}(2)_{\mathrm{FCD}}$ and $\mathrm{Sp}(4)_{\mathrm{FCD}}$. For $\mathrm{SU}(2)_{\mathrm{FCD}}$, which corresponds to two weak doublets, a substantial overlap exists, pointing to couplings to gauge bosons that are larger than the SM values. These effects should become measurable once more precise data on the Higgs couplings are available. The intersection becomes smaller for $\mathrm{Sp}(4)_{\mathrm{FCD}}$, which has 4 doublets, while larger $\mathrm{Sp}(N)_{\mathrm{FCD}}$ are clearly disfavored as EWPTs push the parameters in a region excluded by the Higgs coupling measurements. Our results clearly show that the TC limit is still allowed, provided that the correct value of the mass can be achieved.

[9]A lighter mass can be achieved by considering underlying dynamics that is not QCD-like [18,80], or a near-conformal one [19,81]. This situation can be achieved in the model under consideration by adding a small number of fermions in the adjoint representation [30] of $\mathrm{SU}(2)_{\mathrm{FCD}}$.

C. General case

We now turn our attention to the general case. To reduce the number of unknown parameters, we fix the σ couplings as follows: $\tilde{\kappa}_G = \tilde{\kappa}_t = \tilde{\kappa}$. We also fix the mass of the heavier Higgs h_2 and plot the bounds in the plane θ–α. In Fig. 3, we show the bounds in the case $\tilde{\kappa} = 1$, and $m_{h_2} = 1$ TeV. The plot shows a degeneracy in the bounds from the Higgs couplings due to the fact that the couplings of both the light and heavy Higgses depend only on the difference $(\theta - \alpha)$. On the other hand, EWPTs, in absence of any near-conformal dynamics [62] or sources of isospin breaking, as it is well known do prefer small θ cutting out the TC corner. Interestingly, however, we observe a novel way to loosen the bound on θ, thanks to a positive mixing angle α allowing for values of θ up to $\pi/4$. This is an interesting result since it would reduce the level of fine-tuning needed to achieve either a pure pNGB or TC limit.

The situation is qualitatively different for values of $\tilde{\kappa}$ different from 1, as shown in Figs. 4 and 5. For couplings smaller than unity, the allowed regions shrink, as the contribution of the heavy Higgs, which tends to compensate for the modification of the Higgs couplings, becomes less important. For larger couplings $\tilde{\kappa} > 1$, the situation is very different: the EWPT allowed regions expand until the TC limit is reached, while the Higgs coupling bounds tend to shrink. In Fig. 5, drawn for $\tilde{\kappa} = 1.1$, we see that the TC limit is allowed. Going to even larger values, for example $\tilde{\kappa} = 1.2$ the TC limit is at odds with the measurements of

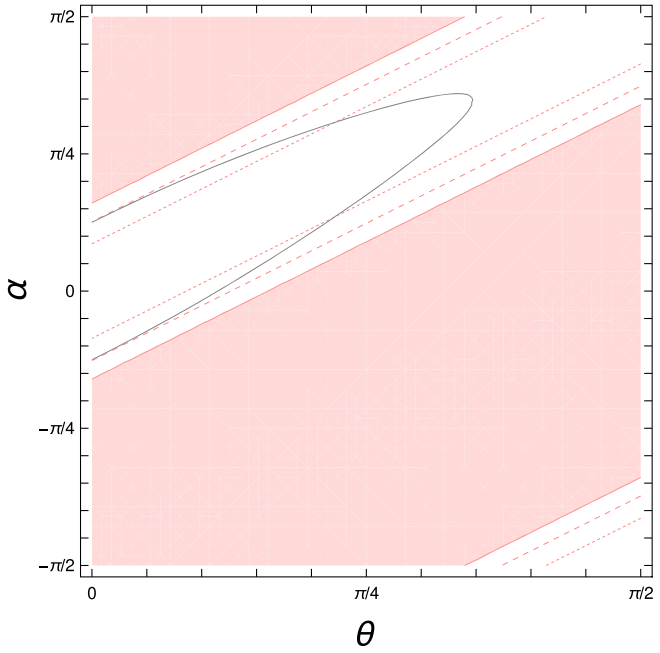

FIG. 3. Region allowed by the Higgs couplings for $\tilde{\kappa} = 1$ and $m_{h_2} = 1$ TeV. The black line indicates the 3σ bound from EWPTs in the $\mathrm{SU}(2)_{\mathrm{FCD}}$.

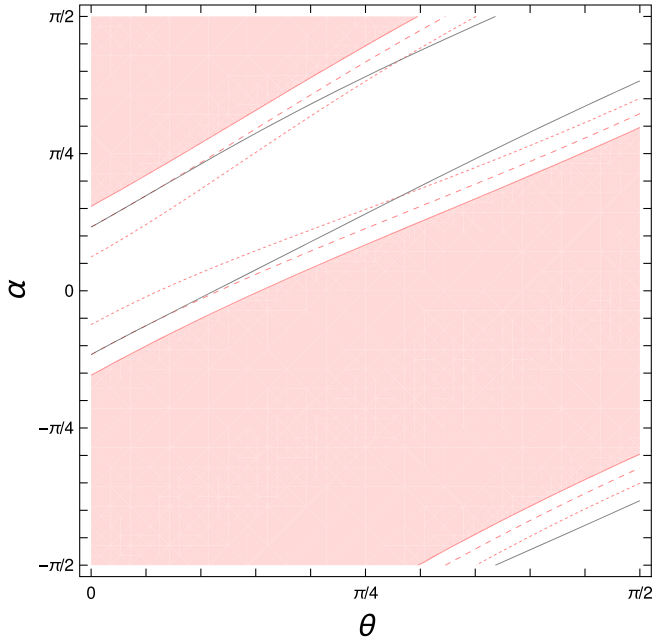

FIG. 5. Region allowed by the Higgs couplings for $\tilde{\kappa} = 1.1$ and $m_{h_2} = 1$ TeV. The black line indicates the 3σ bound from EWPTs in the $\mathrm{SU}(2)_{\mathrm{FCD}}$.

the Higgs couplings but not with EWPTs. This is due, however, to our choice of $\tilde{\kappa}_G = \tilde{\kappa}_t$. We have shown in the previous section that smaller values of $\tilde{\kappa}_t$ would reconcile the Higgs couplings with the experimental measurements.

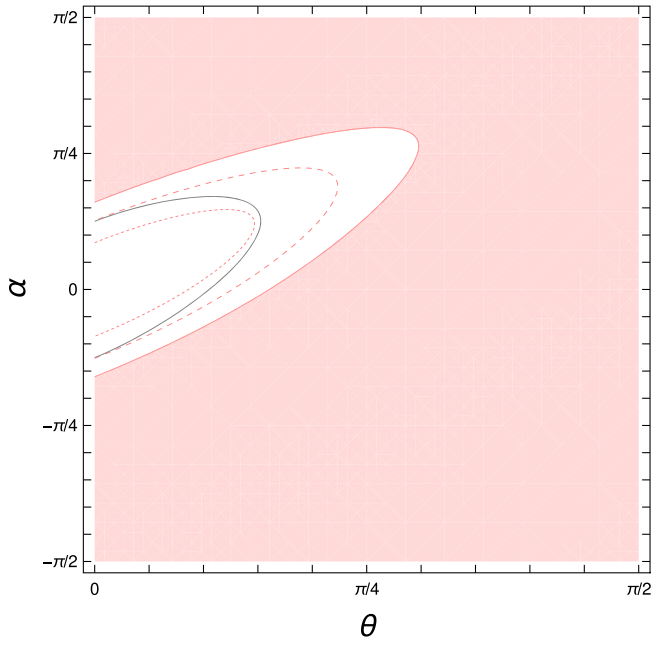

FIG. 4. Region allowed by the Higgs couplings for $\tilde{\kappa} = 0.8$ and $m_{h_2} = 1$ TeV. The black line indicates the 3σ bound from EWPTs in the $\mathrm{SU}(2)_{\mathrm{FCD}}$.

IV. CONSTRAINTS ON THE HEAVIER HIGGS BOSON

In the previous sections we have investigated the implications of the Higgs boson measurements and of the electroweak precision parameters on a general fundamental composite electroweak dynamics, embracing both the ideas of a pNGB Higgs and of a composite Higgs in terms of technifermions. However, the simplest fundamental dynamics we used as a guiding example predicts the existence of other composite states. Preliminary lattice results indicate that the composite vector and axial-vector states are expected rather heavy and outside the present reach of the LHC (see for example [34]). Concerning the scalar sector of the model, lattice results are still too preliminary [65], but a first indication is that the scalar composite σ will be lighter. Furthermore, if the theory has a conformal phase above the condensation scale, induced by additional heavy fermions, the σ can become very light. Inspired by these considerations, we will consider the case where the heavier mass eigenstate h_2 [see Eq. (25)] resulting from the mixing of the pNGB and techni-Higgs may well be within the reach of the LHC. In the effective Lagrangian description, this second heavier Higgs h_2 can be characterized in terms of five parameters: the angles α and θ, the (properly normalized) σ couplings $\tilde{\kappa}_G$ and $\tilde{\kappa}_t$, and the mass m_{h_2}. The couplings of h_2 to SM gauge bosons $V = W^{\pm}, Z$, and the fermions (mainly the top) are given by:

$$\frac{g_{h_2VV}}{g^{\rm SM}_{hVV}} = \sin(\theta-\alpha) + (\tilde{\kappa}_G - 1)\sin\theta\cos\alpha,$$
$$\frac{g_{h_2f\bar{f}}}{g^{\rm SM}_{hf\bar{f}}} = \sin(\theta-\alpha) + (\tilde{\kappa}_t - 1)\sin\theta\cos\alpha. \quad (41)$$

In addition, a potentially large coupling to two light Higgses h_1 is present: it receives contributions of order f from the potential [with nontrivial dependence on the parameters of the effective couplings of σ, see. Eqs. (27)–(29)] together with contributions from derivative couplings from the kinetic term in Eq. (7).

To illustrate the phenomenology of this second Higgs, for simplicity we focus on the decoupling limit $\alpha \to 0$ where $h_2 = \sigma$ and the relevant on-shell coupling to two Higgses (including the kinetic term contribution) is given by

$$g_{\sigma h^2}|_{\rm on-shell} = -\frac{m_h^2}{v}\frac{1}{\sin\theta}(\tilde{\kappa}_m^{(1)}\cos^2\theta - 2\tilde{\kappa}_t\cos(2\theta)) - \frac{\tilde{\kappa}_G\sin\theta}{v}m_\sigma^2\left(1-\frac{2m_h^2}{m_\sigma^2}\right). \quad (42)$$

In Fig. 6 we show a typical plot of the branching ratios for a choice of the parameters: the decays into two Higgs bosons is dominant close to the threshold (driven by the coupling from the potential) and it may be an important channel for LHC searches. The dip around 800 GeV is due to a cancellation with the kinetic coupling, while in the high mass limit (where the kinetic coupling dominates) the channels WW, ZZ, h_1h_1 and $\eta\eta$ have branchings which are in the ratios 2:1:1:1 expected by the equivalence theorem. Varying the parameters does not change the picture qualitatively.

At the LHC, a heavy Higgs is being searched for in many channels: here we focus on the most promising ZZ and hh ones. In Fig. 7 we show the present LHC bounds (at 13 TeV) in the m_{h_2}–θ plane, compared to the electroweak precision bounds. The bounds coming from the heavy Higgs boson $\to ZZ$ [83,84] are in blue (leptons plus missing energy and 4 lepton channels) while those from hh [85,86] are in red ($\gamma\gamma b\bar{b}$ at low mass, and $4b$ at high mass). Remarkably, present LHC bounds are competitive with, if not stronger than, the electroweak precision bounds for masses below 1 TeV. At low mass, the hh, which dominated the branching ratios, is weak because of weaker experimental bounds (except for islands appearing for specific parameter choices).

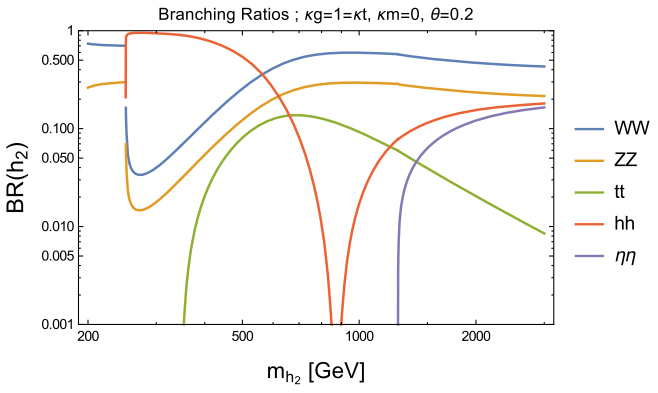

FIG. 6. Branching ratios of h_2 as a function of its mass in the limit $\alpha \to 0$. The plot shows a typical situation, where we chose $\tilde{\kappa}_G = \tilde{\kappa}_t = 1$, $\tilde{\kappa}_m^{(1)} = 0$ and $\theta = 0.2$. The lines correspond to WW (blue), ZZ (orange), $t\bar{t}$ (green), hh (red) and $\eta\eta$ (violet).

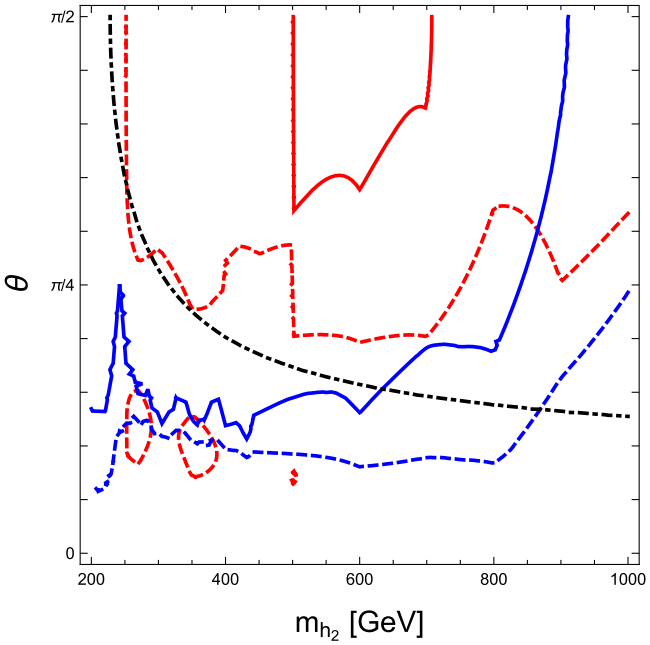

FIG. 7. 95% C.L. limit on θ from the LHC searches for $h_2 \to ZZ$ (in blue) [83,84] and $h_2 \to h_1h_1$ (red) [85,86]. The couplings are chosen to $\tilde{\kappa}_G = 1.2$ and $\tilde{\kappa}_m^{(1)} = 0$, while $\tilde{\kappa}_t = 1$ for the solid curves and $\tilde{\kappa}_t = 2$ for the dashed lines. For comparison, the dotted dashed line shows the limit given by EW precision tests. The allowed region for θ lies below the curves (and outside the islands).

V. ADDITIONAL PNGBS: THE SINGLET η

The presence of additional light pNGB scalars is a generic prediction of this class of models. In the minimal case, besides the Higgs boson and the eaten Goldstones, only one gauge singlet η is present. In less minimal cases, based on a FCD model, additional scalars are also predicted (see for instance [25,57,87,88]): however, a singlet with properties very close to the η is always present. It is therefore important to study its phenomenology as a generic prediction of this class of models. It should be stressed that such a state may be absent in effective models based on symmetry breaking patterns not related to a FCD, as for instance in [89,90].

The singlet state has peculiar properties compared to the other pNGBs (i.e. the Higgs and the Goldstone bosons eaten by the $W^{\pm}$ and Z). The effective Lagrangian for the pNGBs in Eq. (7) does not contain any coupling with an odd number of η fields, thus showing an apparent symmetry

$$\eta \to -\eta \tag{43}$$

that would prevent the η from decaying. At the level of the Goldstone matrix Σ, this symmetry transformation can be expressed as

$$\Omega \cdot \Sigma(h,-\eta) \cdot \Omega^T = \Sigma(h,\eta), \qquad \Omega = \begin{pmatrix} & \sigma_2 \\ \sigma_2 & \end{pmatrix}, \tag{44}$$

where Ω is a transformation belonging to the unbroken Sp (4). The action of this transformation on the gauged generators[10] is

$$\Omega^{\dagger} \cdot S_L^i \cdot \Omega = S_R^i, \tag{45}$$

which corresponds to exchanging the generators of $SU(2)_L$ with the generators in $SU(2)_R$. About the top Yukawa, the coupling can be written as:

$$(t_L, b_L, 0, 0) \cdot \Sigma \cdot (0,0,t_R,0)^T \tag{46}$$

and the transformation rules are

$$(t_L, b_L, 0, 0) \cdot \Omega = (0,0,-ib_L, it_L), \tag{47}$$

$$\Omega^T \cdot (0,0,t_R,0) = (0, it_R, 0, 0), \tag{48}$$

where the $\mathrm{SU}(2)_L$ doublet is transformed into an $\mathrm{SU}(2)_R$ antidoublet, and same for the incomplete $\mathrm{SU}(2)_R$ doublet containing t_R. This exchange is compatible with the exchange between the $\mathrm{SU}(2)_L$ and $\mathrm{SU}(2)_R$ generators, seen above. The elementary fermions also pick up a complex phase, which is not physically relevant.

The parity changing sign to η can, therefore, be though of as a systematic exchange of the two SU(2)'s, and this does not change the physical couplings of the pNGB Higgs h nor of η, at the level of the leading order Lagrangian. The reason for this is that η is a singlet, while h couples to the symmetry breaking which is invariant under the exchange (being custodial invariant).

[10]In fact, the off-diagonal blocks can contain any linear combination of the 3 Pauli matrices: we chose σ_2 because it allows for simpler transformation properties on the gauged generators of SU(4).

The action of Ω on the mass term M_Q in Eq. (3) reads:

$$\Omega^T \cdot M_Q \cdot \Omega = \Omega^T \cdot \begin{pmatrix} \mu_L i\sigma_2 & 0 \\ 0 & \mu_R i\sigma_2 \end{pmatrix} \cdot \Omega = -\begin{pmatrix} \mu_R i\sigma_2 & 0 \\ 0 & \mu_L i\sigma_2 \end{pmatrix}. \tag{49}$$

Once again, the two masses corresponding to the $\mathrm{SU}(2)_L$ and $\mathrm{SU}(2)_R$ doublets are exchanged however with an additional minus sign, i.e. $\mu_{L/R} \to -\mu_{R/L}$. The mass can be split into two terms:

$$M_Q = \frac{\mu_L - \mu_R}{2}\begin{pmatrix} i\sigma_2 & 0 \\ 0 & -i\sigma_2 \end{pmatrix} + \frac{\mu_L + \mu_R}{2}\begin{pmatrix} i\sigma_2 & 0 \\ 0 & +i\sigma_2 \end{pmatrix}. \tag{50}$$

The first term, proportional to Σ_B, is even under the exchange, while the second is odd. From this analysis we can deduce that the only spurion that breaks the η parity explicitly is the second piece of the mass term, thus there will be breaking terms proportional to $\mu_L + \mu_R$. Note that, for the analysis to be consistent, one would expect $\mu_L + \mu_R \ll \mu_L - \mu_R$, else the vacuum would align in a different direction. Additional operators containing linear couplings of the η will be generated at higher order, as we will show below.

A. Linear couplings

The operators generating Yukawa couplings and masses for the SM fermions do not contain linear couplings of the singlet η to fermions. Going one order higher in a spurion expansion, there exists a unique operator which contains a linear η-f-f coupling, generated by the mass and the top Yukawa [31]:

$$\mathcal{O}_1 = (Qt^c)^{\dagger}_{\alpha} \mathrm{Tr}[M_Q \Sigma P^{\alpha} \Sigma] \tag{51}$$

where α, β are $\mathrm{SU}(2)_L$ indices, and M_Q is the mass matrix for the techniquarks in Eq. (3). Expanding,

$$\mathcal{O}_1 = (\mu_L - \mu_R)\cos\theta \sin\theta t_L t_R^c + \frac{1}{2\sqrt{2}f}[h(\mu_L - \mu_R)\cos 2\theta + i\eta(\mu_L + \mu_R)\sin\theta] t_L t_R^c + \ldots, \tag{52}$$

the operator generates a correction to the mass of the top (and coupling of the Higgs), together with a linear coupling of η. Notice that, unsurprisingly, the couplings of the singlet is proportional to the odd combination of masses which do not affect the Higgs potential at the leading order. So, such coupling can be set to zero with the choice $\mu_R = -\mu_L$

without affecting the EW sector of the model. In models with top partners [39], linear couplings can also be generated via appropriate choices of the representation of the top partners [41]. Here we want to point out that linear couplings of η to fermions, which cannot be set to zero, are present at higher orders in the spurion expansion. In order to elucidate this point, let us consider the following operators:

$$\mathcal{O}_2 = (Qt^c)^\dagger_\alpha \sum_i g_i^2 \mathrm{Tr}[S_i \Sigma S_i^* M_Q \Sigma P^\alpha], \tag{53}$$

$$\mathcal{O}_3 = (Qt^c)^\dagger_\alpha \sum_i g_i^2 \mathrm{Tr}[S_i \Sigma S_i^* \Sigma^* M_Q^\dagger P^\alpha], \tag{54}$$

where the sum runs over the gauged generators of SU(4). The structure of the operators suggests that they may arise as one-loop corrections of the EW gauge bosons to the coupling of the elementary fermions to the dynamics, thus we expect their coefficients to be naively suppressed by a loop factor with respect to the one in Eq. (51). Expanding the combination

$$\mathcal{O}_2 - \mathcal{O}_3 = (\mu_L - \mu_R)\left[\frac{3g^2 + g'^2}{16}\left(\sin(2\theta) + \frac{\cos(2\theta)}{\sqrt{2}f}h\right) + i\frac{3g^2 - g'^2}{16\sqrt{2}f}\sin\theta\eta + \ldots\right](t_L t_R^c)^\dagger, \tag{55}$$

we see that it contains a linear coupling of η proportional to the even combination of masses, which cannot therefore be set to zero. This proves that a linear coupling of η to fermions is always generated in this model. Furthermore, as the operators always generate a correction to the mass of the SM fermion, the couplings of the η to light quarks are always naturally suppressed by the SM Yukawa hierarchy. We also note that the linear coupling of η would vanish if an exact $\mathrm{SU}(2)_L$–$\mathrm{SU}(2)_R$ symmetry were imposed on the model by gauging the full $\mathrm{SU}(2)_R$ group: in this limit, the gauge coupling factor would be replaced by $3g^2 - 3g'^2 = 0$, as $g = g'$.

Linear couplings to gauge bosons are generated by the Wess-Zumino-Witten anomaly term, which is always present due to the fermionic nature of the underlying components and violates the η-parity. The correct expression for the couplings can be found in Ref. [31]: notably, no coupling to photons is present. Couplings $\eta \to gg$ and $\eta \to \gamma\gamma$ will however be generated by a top quark loop at the next leading order, after taking into account the η-t-t interaction discussed above. In this model, the $W^\pm$ loop correction to the η-γ-γ coupling vanishes due to presence of the anti-symmetric tensor $\epsilon^{\mu\nu\rho\sigma}$, since there should be no further radiative corrections to the anomalous interaction. These subleading couplings give negligible contribution to the width, however the coupling to gluons may play an important role for production at the LHC.

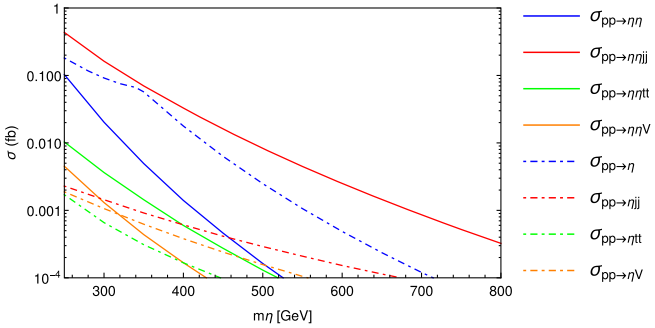

FIG. 8. Production cross sections as a function of m_η at the LHC Run II with $\sqrt{s} = 13$ TeV. We set the PDF to be MSTW2008NLO. The renormalization and factorization scales are fixed to be $\mu_R = \mu_F = \Sigma_f m_f/2$, where we sum over the massive final states. The cross sections of the pair productions are drawn in solid lines while the cross sections of corresponding single productions are drawn in dashed lines with matching colors.

B. Production cross sections

The decay modes of η have already been illustrated in Ref. [31]: below the $t\bar{t}$ threshold, the dominant decays are in gauge bosons via the Wess-Zumino-Witten (WZW) anomalous couplings. Fermionic modes become relevant at large mass, where $t\bar{t}$ dominates, and very low where $b\bar{b}$ start becoming relevant.

To assess the potential at the LHC, however, it is crucial to study the production cross sections. We calculated production rates at leading order via a MadGraph [91] simulation, where the MSTW2008NLO [92] parton distribution functions (PDFs) sets are chosen. We remark that varying the PDF choice would induce a 10% effect, while QCD NLO corrections are expected to give sizeable effects for many of the production channels. The results are shown in Fig. 8 for a center of mass energy of 13 TeV. It is apparent that all production modes gives very small rates, always below 1 fb. The fast drop with increasing mass is due to the PDFs, but also to the fact that for increasing mass (decreasing $\sin\theta$) the couplings of the η are suppressed.

The leading production mechanism is pair production via vector boson fusion (VBF), in solid red in the plot. This process receives a contribution from the quartic couplings, proportional to $\sin\theta$, generated by the lowest order Lagrangian and from s-channel Higgs exchange. The two amplitudes, in fact, interfere constructively. The corresponding single production, due to the WZW couplings, is very small. The next leading processes are due to gluon fusion productions of a single (dashed blue) and a pair (solid blue) of η's. Both processes are induced by a loop of top quarks, and in the numerical simulation we assumed that, for single production, the corresponding operator contributes a maximum of 10% to the top mass. All other channels, like production in association with tops (green) and with a gauge boson (orange) are subleading. The smallness of the production rates clearly imply that this

process can only be accessed at very high luminosity LHC, thus the elusive η is not a good discovery candidate for this class of models. Furthermore, in models where the Higgs potential is stabilised by the techni-fermion mass, the mass of the singlet is correlated to the Higgs mass and the bound on $\theta \lesssim 0.2$ imposes that $m_\eta \gtrsim 600$ GeV, thus pointing to parameter regions where the cross sections are at the level of a few ab. For such large masses, the main decay channel is in a pair of tops, thus a final state with 4 top quarks can be achieved. The presence of two forward jets from the VBF production may help tagging this signal, else the backgrounds (including the SM 4-top production) seem overly dominant. We can thus conclude that detecting the presence of η is extremely difficult at the LHC.

For completeness, we also calculated the production cross section at a linear electron-positron collider. The main channel is the production in association with a neutral boson, i.e. $e^+e^- \to \eta\gamma$ and $e^+e^- \to \eta Z$. Analytical expressions of the cross sections are shown below:

$$\sigma(e^+e^- \to \eta\gamma) = \frac{\alpha g_{\eta Z\gamma}^2 (s - m_\eta^2)^3}{s((s - m_Z^2)^2 + m_Z^2\Gamma_Z^2)} \cdot \frac{((c_w^2 - s_w^2)^2 + 4s_w^4)}{12 c_w^2 s_w^2}, \tag{56}$$

$$\begin{aligned}\sigma(e^+e^- \to \eta Z) &= \frac{\alpha((s - m_\eta^2 - m_Z^2)^2 - 4m_\eta^2 m_Z^2)^{3/2}}{12 s^3((s - m_Z^2)^2 + m_Z^2\Gamma_Z^2) {c_w}^2 {s_w}^2} \\ &\cdot (8 g_{\eta Z\gamma}^2 (s - m_Z^2)^2 c_w^2 s_w^2 + g_{\eta ZZ}^2 s^2((c_w^2 - s_w^2)^2 + 4 s_w^2) \\ &+ 4 g_{\eta Z\gamma} g_{\eta ZZ} s (s - m_Z^2) c_w s_w (c_w^2 - 3 s_w^2)),\end{aligned} \tag{57}$$

where $s > m_\eta^2$ and $s > (m_\eta + m_Z)^2$ respectively. In the case with only SM gauge boson mediation, as in Eqs. (56)–(57), the cross sections increase with the centre of mass energy squared s above the final state threshold, and then flatten to a constant value in the high energy limit. In Fig. 9, we plot the two production cross sections in the large limit $s \gg m_\eta^2$. Due to the smallness of the couplings $g_{\eta Z\gamma}$ and $g_{\eta ZZ}$, the cross sections turn out to be very small and comparable to the relevant results at the hadronic collider.

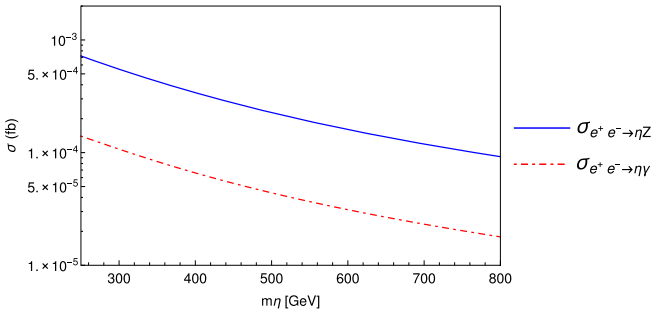

FIG. 9. Production cross sections for the $e^+e^- \to \eta Z$ and $e^+e^- \to \eta\gamma$ from the anomalous $\eta - V - V'$ vertex in the large energy squared limit $s \gg m_\eta^2$.

VI. CONCLUSIONS

The ongoing Run II at the LHC is exploring a higher energy range and will have a chance to help clarifying the structure of the SM and its extensions. Among these extensions the possibility of composite electroweak dynamics is particularly appealing, and it is of paramount importance to have a status of the present constraints coming from the final combined Run I results. We have therefore performed an analysis that encompasses the simplest realizsations bridging composite Goldstone Higgs models and technicolor-like theories focusing on the scalar sector. By simplest we mean that it admits the most minimal fundamental realization, also investigated via first principle lattice investigations.

A typical model of fundamental composite dynamics will contain scalars behaving like pNGBs of the global symmetry breaking and are therefore light scalars that are truly composite states, and spin-1 states. Lattice data seem to indicate that the spin-1 states are always fairly heavy, above 2–3 TeV and with masses increasing for smaller θ parameters. Thus, from this kind of scenario, the states that should be the first ones to be studied at the LHC are scalars. In this work we focused on the minimal fundamental composite dynamics scenario, based on the symmetry breaking SU(4)/Sp(4). Together with a Higgs-like state, the pNGBs also include a singlet η. We showed that the couplings of the singlet correspond to too feeble cross sections to allow for direct probes at the LHC. Thus the only bounds derive from the EWPT constraints on the alignment angle originating from electroweak symmetry breaking. For instance, in the limit where the techni-Higgs decouples, we found a bound on mass $m_\eta \gtrsim 600$ GeV corresponding to $\theta < 0.25$. We have investigated the interesting phenomenological interplay between the pNGB and techni-Higgs interpretation of the discovered Higgs particle. These two states necessarily mix since they are both present in any fundamental four-dimensional realization of a composite pNGB nature of the Higgs. Once the effective Lagrangian has been introduced and properly justified, we used the EWPTs as well as CMS and ATLAS most recent constraints on the Higgs couplings and decays to constrain the effective coupling parameter space. While in the pNGB limit, common to composite Higgs models, we obtain bounds similar to the ones present in the literature, we showed that a less fine tuned vacuum can be reached once a significant mixing between the two scalars is generated. We also studied in detail the TC-limit of the parameter space, where the Higgs is completely identified with the techni-Higgs. This limit requires a tuning in the mass and in the couplings to the gauge bosons which have no known reason to be SM-like: we showed that compatibility with the Higgs couplings and to EWPTs poses

significant constraints on the value of the couplings, and on the rank of the underlying FCD gauge group (Sp($2N$) with $N > 2$ are disfavored). We then investigated the potential phenomenological impact of the singlet pNGB and the heavier Higgs-like state. The η cannot play the role of dark matter as it decays into gauge bosons via the WZW anomaly and to fermions via higher order operators (possibly generated by electroweak loops). We also consider the quark loop induced decay of η into gluon pair and diphoton, although these modes are subleading. However, the production rates at the LHC Run II, and at a future linear collider, are very small, making its detection very challenging. The second Higgs may also show up in searches for Higgs-like states at high mass, and we showed that the present bounds are quite mild allowing for masses of a few hundred GeV. This study can be considered as a benchmark for models of fundamental composite dynamics: nonminimal cases may contain more scalars with better detection prospects as they may be charged, while others may play the role of dark matter.

We have shown that the first LHC run is compatible with a composite nature of the Higgs mechanism in any of the limits considered, including the technicolor-like setup. Because of the link to the fundamental dynamics, we will be able, in the near future, to relate these constraints to direct first principle lattice simulations. Our results set the stage for the LHC Run II searches of composite dynamics at the Fermi scale.

ACKNOWLEDGMENTS

We wish to thank M. Gillioz for useful discussion, and J. B. Flament for providing us the updated code fitting the ellipses from signal strength measurements. A. D. is partially supported by Institut Universitaire de France. We also acknowledge partial support from the Labex-LIO (Lyon Institute of Origins) under Grant No. ANR-10-LABX-66 and FRAMA (FR3127, Fédération de Recherche "André Marie Ampère"), the Danish National Research Foundation under the Grant No. DNRF 90 and the Institut Français du Danemark.

[1] D. B. Kaplan and H. Georgi, SU(2) × U(1) breaking by vacuum misalignment, Phys. Lett. **136B**, 183 (1984).
[2] D. B. Kaplan, H. Georgi, and S. Dimopoulos, Composite Higgs scalars, Phys. Lett. **136B**, 187 (1984).
[3] G. Cacciapaglia and F. Sannino, Fundamental composite (Goldstone) Higgs dynamics, J. High Energy Phys. 04 (2014) 111.
[4] S. Weinberg, Implications of dynamical symmetry breaking, Phys. Rev. D **13**, 974 (1976).
[5] L. Susskind, Dynamics of spontaneous symmetry breaking in the Weinberg-Salam theory, Phys. Rev. D **20**, 2619 (1979).
[6] F. Sannino, Conformal dynamics for TeV physics and cosmology, Acta Phys. Pol. B **40**, 3533 (2009).
[7] N. D. Christensen and R. Shrock, Technifermion representations and precision electroweak constraints, Phys. Lett. B **632**, 92 (2006).
[8] H. S. Fukano and F. Sannino, Conformal window of gauge theories with four-fermion interactions and ideal walking, Phys. Rev. D **82**, 035021 (2010).
[9] J. A. Evans, J. Galloway, M. A. Luty, and R. A. Tacchi, Flavor in minimal conformal technicolor, J. High Energy Phys. 04 (2011) 003.
[10] R. Foadi, M. T. Frandsen, and F. Sannino, 125 GeV Higgs boson from a not so light technicolor scalar, Phys. Rev. D **87**, 095001 (2013).
[11] A. L. Fitzpatrick, G. Perez, and L. Randall, Flavor Anarchy in a Randall-Sundrum Model with 5D Minimal Flavor Violation and a Low Kaluza-Klein Scale, Phys. Rev. Lett. **100**, 171604 (2008).
[12] M. E. Albrecht, M. Blanke, A. J. Buras, B. Duling, and K. Gemmler, Electroweak and flavour structure of a warped extra dimension with custodial protection, J. High Energy Phys. 09 (2009) 064.
[13] A. Parolini, Phenomenological aspects of supersymmetric composite Higgs models, Phys. Rev. D **90**, 115026 (2014).
[14] R. Rattazzi, V. S. Rychkov, E. Tonni, and A. Vichi, Bounding scalar operator dimensions in 4D CFT, J. High Energy Phys. 12 (2008) 031.
[15] V. S. Rychkov and A. Vichi, Universal constraints on conformal operator dimensions, Phys. Rev. D **80**, 045006 (2009).
[16] O. Antipin, E. Mø lgaard, and F. Sannino, Higgs critical exponents and conformal bootstrap in four dimensions, J. High Energy Phys. 06 (2015) 030.
[17] A. Vichi, Improved bounds for CFT's with global symmetries, J. High Energy Phys. 01 (2012) 162.
[18] F. Sannino and K. Tuominen, Orientifold theory dynamics and symmetry breaking, Phys. Rev. D **71**, 051901 (2005).
[19] D. D. Dietrich and F. Sannino, Conformal window of SU(N) gauge theories with fermions in higher dimensional representations, Phys. Rev. D **75**, 085018 (2007).
[20] F. Sannino, Conformal windows of SP(2N) and SO(N) gauge theories, Phys. Rev. D **79**, 096007 (2009).
[21] E. Poppitz and M. Unsal, Conformality or confinement: (IR) relevance of topological excitations, J. High Energy Phys. 09 (2009) 050.
[22] N. Chen, T. A. Ryttov, and R. Shrock, Patterns of dynamical gauge symmetry breaking, Phys. Rev. D **82**, 116006 (2010).
[23] T. A. Ryttov and R. Shrock, Infrared evolution and phase structure of a gauge theory containing different fermion representations, Phys. Rev. D **81**, 116003 (2010); Erratum, Phys. Rev. D **82**, 059903(E) (2010).

[24] T. A. Ryttov and R. Shrock, Generational structure of models with dynamical symmetry breaking, Phys. Rev. D **81**, 115013 (2010).
[25] M. J. Dugan, H. Georgi, and D. B. Kaplan, Anatomy of a composite Higgs model, Nucl. Phys. **B254**, 299 (1985).
[26] R. Contino, Y. Nomura, and A. Pomarol, Higgs as a holographic pseudoGoldstone boson, Nucl. Phys. **B671**, 148 (2003).
[27] R. Contino, The Higgs as a composite Nambu-Goldstone boson, arXiv:1005.4269.
[28] B. Bellazzini, C. Csaki, and J. Serra, Composite Higgses, Eur. Phys. J. C **74**, 2766 (2014).
[29] G. Panico and A. Wulzer, The composite Nambu-Goldstone Higgs, Lect. Notes Phys. **913**, 1 (2016).
[30] T. A. Ryttov and F. Sannino, Ultra minimal technicolor and its dark matter TIMP, Phys. Rev. D **78**, 115010 (2008).
[31] J. A. Evans, J. Galloway, M. A. Luty, and R. A. Tacchi, Minimal conformal technicolor and precision electroweak tests, J. High Energy Phys. 10 (2010) 086.
[32] R. Lewis, C. Pica, and F. Sannino, Light asymmetric dark matter on the lattice: SU(2) technicolor with two fundamental flavors, Phys. Rev. D **85**, 014504 (2012).
[33] A. Hietanen, R. Lewis, C. Pica, and F. Sannino, Composite Goldstone dark matter: Experimental predictions from the lattice, J. High Energy Phys. 12 (2014) 130.
[34] A. Hietanen, R. Lewis, C. Pica, and F. Sannino, Fundamental composite Higgs dynamics on the lattice: SU(2) with two flavors, J. High Energy Phys. 07 (2014) 116.
[35] R. Arthur, V. Drach, M. Hansen, A. Hietanen, C. Pica, and F. Sannino, SU(2) gauge theory with two fundamental flavors: A minimal template for model building, Phys. Rev. D **94**, 094507 (2016).
[36] G. Aad *et al.* (ATLAS Collaboration), Search for high-mass dilepton resonances in pp collisions at $\sqrt{s} = 8$ TeV with the ATLAS detector, Phys. Rev. D **90**, 052005 (2014).
[37] P. Batra and Z. Chacko, Symmetry breaking patterns for the little Higgs from strong dynamics, Phys. Rev. D **77**, 055015 (2008).
[38] P. Di Vecchia and F. Sannino, The physics of the θ-angle for composite extensions of the standard model, Eur. Phys. J. Plus **129**, 262 (2014).
[39] J. Barnard, T. Gherghetta, and T. S. Ray, UV descriptions of composite Higgs models without elementary scalars, J. High Energy Phys. 02 (2014) 002.
[40] E. Katz, A. E. Nelson, and D. G. E. Walker, The intermediate Higgs, J. High Energy Phys. 08 (2005) 074.
[41] B. Gripaios, A. Pomarol, F. Riva, and J. Serra, Beyond the minimal composite Higgs model, J. High Energy Phys. 04 (2009) 070.
[42] S. R. Coleman, J. Wess, and B. Zumino, Structure of phenomenological Lagrangians. I, Phys. Rev. **177**, 2239 (1969); C. G. Callan, Jr., S. R. Coleman, J. Wess, and B. Zumino, Structure of phenomenological Lagrangians. II, Phys. Rev. **177**, 2247 (1969).
[43] T. Appelquist, P. S. Rodrigues da Silva, and F. Sannino, Enhanced global symmetries and the chiral phase transition, Phys. Rev. D **60**, 116007 (1999).
[44] Z. y. Duan, P. S. Rodrigues da Silva, and F. Sannino, Enhanced global symmetry constraints on epsilon terms, Nucl. Phys. **B592**, 371 (2001).
[45] G. Cacciapaglia and F. Sannino, An ultraviolet chiral theory of the top for the fundamental composite (Goldstone) Higgs, Phys. Lett. B **755**, 328 (2016).
[46] F. Sannino, A. Strumia, A. Tesi, and E. Vigiani, Fundamental partial compositeness, J. High Energy Phys. 11 (2016) 029.
[47] R. Contino, M. Ghezzi, M. Moretti, G. Panico, F. Piccinini, and A. Wulzer, Anomalous couplings in double Higgs production, J. High Energy Phys. 08 (2012) 154.
[48] T. Alanne, H. Gertov, F. Sannino, and K. Tuominen, Elementary Goldstone Higgs boson and dark matter, Phys. Rev. D **91**, 095021 (2015).
[49] O. Matsedonskyi, G. Panico, and A. Wulzer, Light top partners for a light composite Higgs, J. High Energy Phys. 01 (2013) 164.
[50] E. Eichten and K. D. Lane, Dynamical breaking of weak interaction symmetries, Phys. Lett. **90B**, 125 (1980).
[51] D. B. Kaplan, Flavor at SSC energies: A new mechanism for dynamically generated fermion masses, Nucl. Phys. **B365**, 259 (1991).
[52] O. Matsedonskyi, On flavour and naturalness of composite Higgs models, J. High Energy Phys. 02 (2015) 154.
[53] G. Cacciapaglia, H. Cai, T. Flacke, S. J. Lee, A. Parolini, and H. Serodio, Anarchic Yukawas and top partial compositeness: The flavour of a successful marriage, J. High Energy Phys. 06 (2015) 085.
[54] G. Panico and A. Pomarol, Flavor hierarchies from dynamical scales, J. High Energy Phys. 07 (2016) 097.
[55] G. Ferretti and D. Karateev, Fermionic UV completions of Composite Higgs models, J. High Energy Phys. 03 (2014) 077.
[56] G. Ferretti, Gauge theories of partial compositeness: Scenarios for Run-II of the LHC, J. High Energy Phys. 06 (2016) 107.
[57] L. Vecchi, A "dangerous irrelevant" UV-completion of the composite Higgs, arXiv:1506.00623.
[58] C. Pica and F. Sannino, Anomalous dimensions of conformal baryons, Phys. Rev. D **94**, 071702 (2016).
[59] D. Buarque Franzosi, G. Cacciapaglia, H. Cai, A. Deandrea, and M. Frandsen, Vector and axial-vector resonances in composite models of the Higgs boson, J. High Energy Phys. 11 (2016) 076.
[60] M. Golterman and Y. Shamir, Top quark induced effective potential in a composite Higgs model, Phys. Rev. D **91**, 094506 (2015).
[61] R. C. Brower, A. Hasenfratz, C. Rebbi, E. Weinberg, and O. Witzel, Composite Higgs model at a conformal fixed point, Phys. Rev. D **93**, 075028 (2016).
[62] T. Appelquist and F. Sannino, The physical spectrum of conformal SU(N) gauge theories, Phys. Rev. D **59**, 067702 (1999).
[63] F. Sannino, Mass deformed exact S-parameter in conformal theories, Phys. Rev. D **82**, 081701 (2010).
[64] M. E. Peskin and T. Takeuchi, Estimation of oblique electroweak corrections, Phys. Rev. D **46**, 381 (1992).
[65] R. Arthur, V. Drach, M. Hansen, A. Hietanen, R. Lewis, C. Pica, and F. Sannino, Composite (Goldstone) Higgs dynamics on the lattice: Spectrum of SU(2) gauge theory with two fundamental fermions, *Proc. Sci.*, LATTICE2014 (2014) 249 [arXiv:1412.7302].

[66] V. Khachatryan *et al.* (CMS Collaboration), Precise determination of the mass of the Higgs boson and tests of compatibility of its couplings with the standard model predictions using proton collisions at 7 and 8 TeV, Eur. Phys. J. C **75**, 212 (2015).

[67] G. Aad *et al.* (ATLAS Collaboration), Search for the $b\bar{b}$ decay of the standard model Higgs boson in associated $(W/Z)H$ production with the ATLAS detector, J. High Energy Phys. 01 (2015) 069.

[68] G. Aad *et al.* (ATLAS Collaboration), Measurements of Higgs boson production and couplings in the four-lepton channel in pp collisions at center-of-mass energies of 7 and 8 TeV with the ATLAS detector, Phys. Rev. D **91**, 012006 (2015).

[69] G. Aad *et al.* (ATLAS Collaboration), Observation and measurement of Higgs boson decays to WW* with the ATLAS detector, Phys. Rev. D **92**, 012006 (2015).

[70] G. Aad *et al.* (ATLAS Collaboration), Evidence for the Higgs-boson Yukawa coupling to tau leptons with the ATLAS detector, J. High Energy Phys. 04 (2015) 117.

[71] G. Aad *et al.* (ATLAS Collaboration), Measurement of Higgs boson production in the diphoton decay channel in pp collisions at center-of-mass energies of 7 and 8 TeV with the ATLAS detector, Phys. Rev. D **90**, 112015 (2014).

[72] G. Aad *et al.* (ATLAS and CMS Collaborations), Measurements of the Higgs boson production and decay rates and constraints on its couplings from a combined ATLAS and CMS analysis of the LHC pp collision data at $\sqrt{s} = 7$ and 8 TeV, J. High Energy Phys. 08 (2016) 045.

[73] G. Cacciapaglia, A. Deandrea, G. D. La Rochelle, and J. B. Flament, Higgs couplings beyond the standard model, J. High Energy Phys. 03 (2013) 029.

[74] J. B. Flament, Higgs couplings and BSM physics: Run I legacy constraints, arXiv:1504.07919.

[75] M. Baak, J. Cúth, J. Haller, A. Hoecker, R. Kogler, K. Mönig, M. Schott, and J. Stelzer (Gfitter Group Collaboration), The global electroweak fit at NNLO and prospects for the LHC and ILC, Eur. Phys. J. C **74**, 3046 (2014).

[76] R. Barbieri, B. Bellazzini, V. S. Rychkov, and A. Varagnolo, The Higgs boson from an extended symmetry, Phys. Rev. D **76**, 115008 (2007).

[77] R. Contino and M. Salvarezza, One-loop effects from spin-1 resonances in composite Higgs models, J. High Energy Phys. 07 (2015) 065.

[78] D. Ghosh, M. Salvarezza, and F. Senia, Extending the analysis of electroweak precision constraints in composite Higgs models, Nucl. Phys. **B914**, 346 (2017).

[79] C. Grojean, O. Matsedonskyi, and G. Panico, Light top partners and precision physics, J. High Energy Phys. 10 (2013) 160.

[80] D. K. Hong, S. D. H. Hsu, and F. Sannino, Composite Higgs from higher representations, Phys. Lett. B **597**, 89 (2004).

[81] D. D. Dietrich, F. Sannino, and K. Tuominen, Light composite Higgs from higher representations versus electroweak precision measurements: Predictions for CERN LHC, Phys. Rev. D **72**, 055001 (2005).

[82] A. Belyaev, M. S. Brown, R. Foadi, and M. T. Frandsen, The technicolor Higgs in the light of LHC data, Phys. Rev. D **90**, 035012 (2014).

[83] The ATLAS Collaboration, Report No. ATLAS-CONF-2016-056.

[84] The ATLAS Collaboration, Report No. ATLAS-CONF-2016-079.

[85] G. Aad *et al.* (ATLAS Collaboration), Searches for Higgs boson pair production in the $hh \to bb\tau\tau$, $\gamma\gamma WW^*$, $\gamma\gamma bb$, $bbbb$ channels with the ATLAS detector, Phys. Rev. D **92**, 092004 (2015).

[86] V. Khachatryan *et al.* (CMS Collaboration), Search for two Higgs bosons in final states containing two photons and two bottom quarks in proton-proton collisions at 8 TeV, Phys. Rev. D **94**, 052012 (2016).

[87] G. Cacciapaglia, H. Cai, A. Deandrea, T. Flacke, S. J. Lee, and A. Parolini, Composite scalars at the LHC: The Higgs, the sextet and the octet, J. High Energy Phys. 11 (2015) 201.

[88] G. Ferretti, UV completions of partial compositeness: The case for a SU(4) gauge group, J. High Energy Phys. 06 (2014) 142.

[89] J. Mrazek, A. Pomarol, R. Rattazzi, M. Redi, J. Serra, and A. Wulzer, The other natural two Higgs doublet model, Nucl. Phys. **B853**, 1 (2011).

[90] E. Bertuzzo, T. S. Ray, H. de Sandes, and C. A. Savoy, On composite two Higgs doublet models, J. High Energy Phys. 05 (2013) 153.

[91] J. Alwall, M. Herquet, F. Maltoni, O. Mattelaer, and T. Stelzer, MadGraph 5: Going beyond, J. High Energy Phys. 06 (2011) 128.

[92] A. D. Martin, W. J. Stirling, R. S. Thorne, and G. Watt, Parton distributions for the LHC, Eur. Phys. J. C **63**, 189 (2009).